Analogy in the processes of heat exchange of capillary-porous coatings in energy installations

Alexander Genbach[1], *David* Bondartsev[1,], *Iliya* Iliev[2], and *Angel* Terziev[3,*]

[1] Almaty University of Power Engineering & Telecommunications, Almaty, Republic of Kazakhstan
[2] Dept. of Thermotechnics, Hydraulic and Ecology, University of Ruse, Ruse, Bulgaria
[3] Dept. of Power Engineering and Power Machines, Technical University of Sofia, Sofia, Bulgaria

Abstract. A model of the dynamics of steam bubbles generating on a solid surface in porous structures and a steam-generating wall (substrate) is developed. The model is based on the filming and photography with speed camera SKS-1M. The removal of high heat fluxes (up to $2x10^6$ W/m^2) is provided by the combined action of capillary and mass forces with application of intensifiers. An analytical model is developed based on the theory of thermoelasticity. The limiting state of a poorly heat-conducting porous coating and a metal substrate has been determined. The heat fluxes were calculated from the time of spontaneous appearance of the steam nucleation (10^{-8}) up to the time of material destruction ($10^2 \div 10^3$ s). The destruction of the coating under the action of compression forces occurs in much earlier time than the tension forces. The intervals of the heat flux within which such destruction occurs are different for the quartz coating $q_{max} \approx 7x10^7$ W/m^2, $q_{min} \approx 8x10^4$ W/m^2 and for granite coating $q_{max} \approx 1x10^7$ W/m^2, $q_{min} \approx 21x10^4$ W/m^2. Experimental units, experimental conditions, the results of the heat exchange crisis and the limiting state of the surface are presented, and critical heat fluxes are calculated. The investigated capillary-porous system, operating under the combined action of capillary and mass forces, has the advantage over pool boiling, thin-film evaporators and heat pipes.

1 Introduction

The research of the thermohydraulic characteristics of the liquid boiling process in capillary-porous structures was performed with the help of a high-speed camera from the beginning of explosive nucleation of the vapor phase [1] until its destruction. This allowed to develop models and the mechanism of heat transfer and to obtain simple calculated relations for different boiling regimes up to the crisis state [2]. The control of heat transfer due to the combined effect of capillary and mass forces is a base for design of various heat exchange devices.

The visualization of the thermal impact was also realized with the help of holography, which allowed to investigate the limiting state of good and poor heat-conducting materials in the form of porous structures and a steam generating surface. The heat exchange control in porous structures was performed by affecting the internal boiling characteristics and integrated magnitudes [1-4].

It is of interest to give a comparative evaluation of the proposed new capillary-porous cooling system using the combined action of capillary and mass forces with traditional systems: pool boiling, thin-film evaporators and heat pipes [12-15].

The authors [5] make a comparative analysis of heat transfer calculating from the boiling of water with underheating in vertical channels, considering corrosion phenomena to be analogous to the capillary-porous structure [6,7]. However, no studies of heat transfer through a regular structured surface have been performed, besides, the role of the velocity and underheating of the liquid on the boiling crippling in porous coatings is not clear.

According to [8,9], surface boiling on porous surfaces can influence the corrosion, possibly erosion, and the surface strength during bubble collapse in the underheated liquid. Therefore, it is required to investigate the heat transfer in terms of mass and capillary forces, taking into account the liquid excess.

A number of experimental units have been developed which provide a means of studying the integral characteristics of heat transfer: heat flux rate q, liquid and steam flow rates ml, ms, temperature field distribution along the height and length of the heat exchange surface [3,4].

Studies are performed in a capillary-porous cooling system, which can operate on the principle of a closed or non-closed evaporative condensation scheme. Various heat exchange conditions, such as: the method of cooler supplying, the degree of clamping by the capillary-porous structure, the ability to feed the structure from the micro-arteries on the height of the heat exchange surface, the orientation of the wall relative to the gravitational forces, the flat, tubular and curved cooling surfaces, the system operation under pressure until the crisis phenomena with a burn walls are studied in [3,4].

* Corresponding author: aterziev@tu-sofia.bg

Holography methods [16], dimensional analysis [2] and analogous phenomena [3-4] generalization have been used to study the mechanism of heat transfer.

The heat exchange and internal characteristics are controlled by elliptical systems [1], with the combined action of capillary and mass forces.

The pressure effect on the intensity of heat transfer in porous systems was investigated in [1,16].

It is of interest to compare the intensity of heat transfer and the limiting state of the surface (boiling crisis) with heat pipes [10,11], and also to assess the possibilities of the mechanics of the destruction of heating (cooling) surfaces covered by capillary-porous structures with respect to strength, resource tasks and justification of safety operation of thermal mechanical power equipment of power plants [12-15]. The modernization and extension of the useful lifetime of gas turbine and steam turbine power plants continue to be a pressing issue for a long time.

2 Experimental study the heat transfer crisis and the limiting state of the cooling (heating) surface, covered with a capillary-porous structure

We have developed and investigated experimental installations for determining the integral (average) heat-exchange characteristics of a capillary-porous cooling system; the functioning scheme and a measuring procedure, the device of a cooling element with tubular arteries perforated pressure plate and microarriers have been prepared. Various factors have been studied: the height of the heat exchange surface, the pressure in the cooling system, up to the wall burnt and wicks (Fig. 1 and 2).

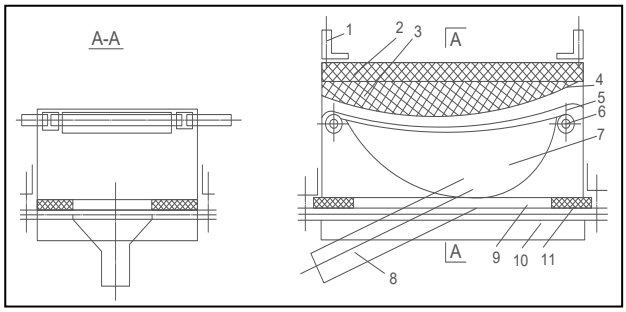

Fig. 1. The scheme of the experimental unit with curved surface, operating under high pressure: 1 – electrode; 2 – asbestos board; 3 – flaked asbestos; 4 – nichrome; 5 – grid structure; 6 – liquid supply pipe; 7 – steam channel; 8 – steam branch pipe; 9 – body; 10 – cover; 11 – gasket.

The main heater is supplied with electric power from a welding transformer of the TSD-1000 type with the following fixed values of the output voltage: 2,5; 5; 7,5 and 10. The electric current supplying the heater is measured with a universal transformer of the UTT-6M2 0,2 class type, according to the scheme. The secondary current is up to 5 amperes; the primary current is 100...2000 amperes. The voltage drop on the heater is measured by a voltmeter of the D523 0.5 class type. The maximum possible error of current measurement is ± 0.6%, of the voltage drop is ± 1%, and of the power is ± 1.6%. Electric energy is applied to the guarding heater from the voltage regulator of the RNO type.

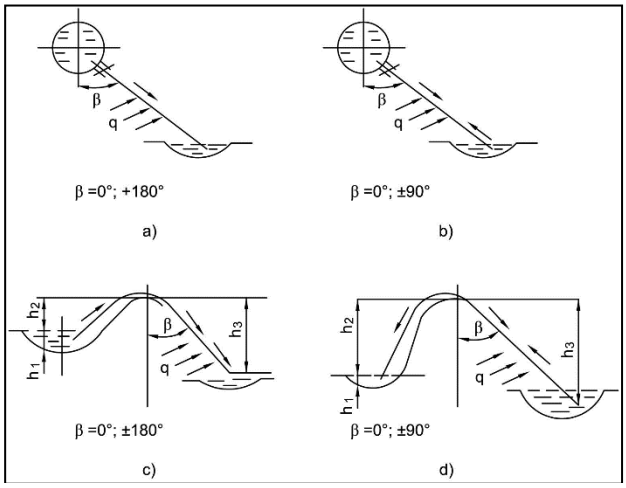

Fig. 2. Scheme for the study of the heat-release surface orientation: a, b – liquid is supplied by the artery; c, d – the "siphon" liquid supply: β is the angle between the cooling surface and the gravitational force.

The current transformer of the TSD-1000 type with 71V off-load output voltage is used when studying the starting point of liquids boiling and critical loads, the current strength is regulated within the limits of 200...1200 amperes. Liquid temperature and ambient temperature are measured with mercury thermometers TL – 4 with a scale of 0 – 50 °C and 50 – 100 °C and a division value of 0.1 °C.

The liquid drain temperature and the steam temperature are measured with chromel-copel thermocouples made of wire with a diameter of 0,1 mm. The diameter of the junction head of the thermocouple is 0,4 mm. The thermocouple electrodes are isolated with two-channel straws with a diameter of 1 mm, which are fixed with butvar-phenolic adhesive inside injection needles, which have 1,2 mm diameter.

To measure the wall temperature, thermocouples electrodes with a diameter of 0,2 mm are welded to the wall by an electric arc formed during the discharge of condensers. The drilling to a depth of 1,9 mm with diameter of 1,2 mm with an accuracy of ± 0,05 m orthogonal to the wall surface of 2 mm thickness is made to achieve that. The thermocouples electrodes are insulated with porcelain strips with diameter of 1,2 mm and are taken out along the wall surface between two mica layers with a thickness of 0,05 mm, glued to the heater surface.

Cold ends of thermocouples are thermostated in melting ice. The electrodes of thermocouples are connected with two twelve-pointed PP-63 class 0,05 switches. The unit and instruments are grounded to eliminate the effect of induced sneak currents on the thermocouple readings. The flow rates of refrigerating and circulating liquid are determined with electric rotameters of the RED type with a secondary electronic device of the KSDZ 43 class 1 type, calibrated with

volumetric method. The flow rates of the merging liquid and condensate are recorded using a measuring container with a pressure scale of $0{,}5x10^{-3}$ liters, and the filling time is recorded with a stop-watch timer C-P-1b type with 0,1 second division value.

The greatest possible error of liquid flow rate determined with rotameters does not exceed ± 3%, and it does not exceed ± 2% in determining with the volumetric method.

The imbalance of the heat supplied by the current and discarded with circulation and excess water heat with account of Qex does not exceed ± 12%, and according to the heat supplied by the steam in the condenser and the heat discarded to the circulation water it does not exceed ± 11%. The discrepancy in the material balance between the flow rate of the refrigerating liquid, flow rate of the drainage and condensate is no more than ± 10%. The procedure for measuring and processing experimental data was published in previous works [16].

3 The results of the heat transfer crisis in the capillary-porous cooling system

3.1 Model of the capillary-porous structure of the cooling system

We considered the growth of a steam bubble of radius R in a separate cell of the structure (Fig. 3). It was assumed that the heat flux q, which determines the growth of the steam bubble, comes from the heating surface q_1, taking into account the "dry" spot through the microlayer of the liquid under the steam bubble, and part of the heat q_2 is supplied from the superheated liquid surrounding the growing bubble, since the superheating of the liquid in the porous structure can reach large values, which increases the content of liquid adjacent layers enthalpy.

The cooling liquid is transported by the combined action of capillary and mass forces $\Delta P_{g+c.}$ The "dry" spot at the base of the bubble is described by the radius r, which at the moment of bubble separation is proportional to $R_{d.s.} = kR$, where the microlayer of the liquid under the bubble forms an angle α' with sides δ'_o and δ_o.

The steam bubble is represented as the volume of the spherical segment, from which the truncated cone formed by the microlayer should be subtracted. The thickness of the micro-layer δ_o that feeds the steam bubble due to its estimation during the growth of the bubble will be constant, since the capillary and gravitational forces allow the fresh portions of the cooling liquid to leak to the base of the bubble. In the steam bubble growth model, there is a direct transition from the developed bubble boiling to the possible onset of the crisis, when the balance of forces breaks down and the thickness of the microlayer tends to zero ($\delta_o \to 0$), which is very important for studying the limiting state of the system.

The interfacial surface 8 and the steam generating wall 4 form a dynamic angle θ average during the time of growth of the steam bubble. Since the problem is solved for not very low pressures, the dynamic processes taking place in the initial stage of the development of the steam bubble are not considered. Then the forces of viscosity and surface tension will also be commensurable with inertial forces and may not be considered.

The emergence of a boiling crisis is associated with an active increase in the size of the "dry" spot at the base of the bubbles.

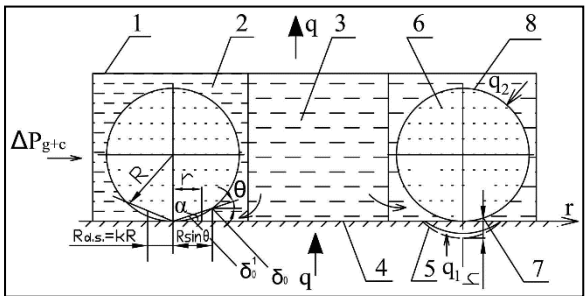

Fig. 3. The model of contact of steam bubbles with a steam generating surface in the cells of steam generation of the porous structure: 1 – skeleton of a porous structure; 2 – cell for generating steam; 3 – cell of a supply with a liquid; 4 – steam generating surface; 5 – front of the propagation of the temperature wave in the volume of the heat-generating surface (stainless steel and copper (dashed line); 6 – steam; 7 – "dry" spot; 8 – front of light (steam) phase propagation.

3.2 Calculation of the boiling crisis

The calculation of q_{cr} in relation to the model (see Fig. 3) can be performed depending on the underheating and the flow velocity according to the equations of work [2], from which it follows that underheating of the liquid allows to expand the heat transfer capabilities in a porous cooling system. Since heat transfer processes take place in thin porous structures, even an insignificant excess of freely flowing film on the outside of the structure, determined by the parameter $\tilde{m}$, at a given hydrostatic pressure ΔP_g and a conditional coefficient of permeability K_f, creates a liquid core from which the underheated cooler will be continuously sucked due to temperature differences and capillary forces.

In addition, the gravitational potential promotes the destruction of steam conglomerates in a porous structure, facilitating the transport of an underheated liquid. The heat flow will be spent additionally on heating of leaking relatively cold portions of liquid.

Excess liquid in the porous system creates a directional flow which leads to deformation of the steam bubbles in the structure, a decrease in their diameter, an increase in the frequency of the formation of bubbles [2]. As the flow velocity increases, the energy expended in displacing liquid from the wall boundary layer increases, and consequently, the generation rate of the steam V_{cr} and the quantity q_{cr} increase. However, at a certain value of the liquid flow rate determined by the parameter $\tilde{m}_{cr}$, the energy expended for extruding liquid from the two-phase wall layer will not be enough, and a heat transfer crisis occurs. Of course, an increase in $q_{cr,v}$ will be achieved with a large flow of liquid, which will lead to an increase in energy losses for the drive of the injection machines.

Upon reaching a certain amount of the water content $\bar{\varphi}'_{cr}$, the flow velocity will not contribute to an increase in q_{cr}, and in some cases may even lead to a decrease in the q_{cr} value, since steam evacuation from the wall zone is difficult. The increase in the velocity of the liquid film adjacent to the wall, due to the parameter $\tilde{m}$, begins to give way to the dominant influence of the fall in the moisture content $\bar{\varphi}'$ in the same zone, which will have a greater effect on q_{cr}, even decreasing it. Therefore, it is required in each separate case to establish an optimal ratio of the excess liquid $\tilde{m}$ depending on the type of the porous structure.

The hydrodynamic model of the liquid boiling crisis in a large volume on the technical surface does not reflect the effect of the thermophysical properties of the wall, although it does occur, which can be explained by the vibrational motion of the steam-liquid interface. This leads to a wavy movement of the heating surface. Therefore, in some places of such surface resonance phenomena should be expected when the wall temperature decreases due to a large selection of steam, which means that the higher the thermal properties of the wall, the more intensive the reduction of the parameter q will be.

For porous cooling systems, for practically all regime and geometric parameters with bubble boiling of water, the depth of penetration of the temperature wave is $h_{av} < \delta_w$, therefore, in the calculated relations for qcr in [1-2], the wall thickness δ_w is not introduced.

Let's present the calculated equation for q_{cr} in the case when $P \geq 0.1$ MPa, and $b_g > 0.28 \times 10^{-3}$ m:

$$q_{cr} = 0.0347\bar{r}\,[g(\rho_l - \rho_s)\rho_s \bar{D}_{\text{br.bub...}}]^{0,5} \left(\frac{b_g}{b_o}\right)^{0,3} \left(\frac{\delta_f}{\delta_o}\right)^{0.5} (1 + cos\beta)^{0.6} \quad (1)$$

where, $\bar{r}$ – heat of vaporization; $\bar{D}_{\text{br.bub...}}$ – average size of a steam conglomerate that meets the condition $\Delta T = \Delta T_{cr}$, determined by the formula of work [2]; $b_o = 0{,}14 \times 10^{-3}$ m; δ_f - structure thickness; $\delta_o = 0{,}18 \times 10^{-3}$m.

It follows from equation (1) that $q_{cr} \sim \bar{D}^{0.5}_{\text{br.bub...}}$ ($p \geq 0.1$ MPa) and $q_{cr} \sim \bar{f}^{0.5}$ ($p < 0.1$ MPa).

Quantity $\bar{D}_{\text{br.bub...}}$ and $\bar{f}$ depend on the thermophysical properties of the heat-dissipating surface: $\bar{D}_{\text{br.bub...}} \sim K_w^{-1}$, $\bar{f}_{cr}^{-1} \sim K_w^2$, where $K_w = I + [(\rho c\lambda)_l/(\rho c\lambda)_w]^{0.5}$. Then for surfaces made of copper and stainless steel and covered with mesh structures, we have the following: $q_{cr} = 1{,}07$ ($p \geq 0{,}1$MPa), $\tilde{q}_{cr} = 1.15$ ($p < 0{,}1$ MPa).

The wall material affects the value of q_{cr} by means of the complex $(\rho c\lambda)_w$, but it is hardly legitimate to say that this is true. It is practically impossible to withstand the same conditions on the purity of the treatment and the microstructure.

When designing the combustion chamber and especially the nozzle, it is necessary to take into account a certain reserve for the thickness of the heating surface. The emergence of the boiling crisis will occur earlier on "thin" heaters, since the size of the "dry" spot in the bottom of the bubbles will begin to increase in the pre-crisis boiling area, the heat exchange process will sharply worsen, the wall temperature will increase. Surfaces that are thicker will require more time for their heating.

For surfaces with a porous coating this issue is especially topical, since in them the bubble growth time is ten times less, the hydrodynamic conditions of the liquid makeup change dramatically and consequently the residence time of the steam near the wall can increase, which eliminates the contact of the liquid with the heat exchange surface, despite the large excess of liquid $\tilde{m}$.

The described process is a prehistory of the development of the boiling crisis. The further "fate" of the process, all other things being equal, is determined by the heat-storage capacity of the heating $(\rho c\lambda)_w$. When the size of the complex is chosen to be large, the probability of prolonging the boiling crisis increases, heat flows along the heating surface will increase, and favorable conditions for the contact of the liquid phase with the wall will again be created. An increase in only the wall thickness by a factor of just a few percent increases the value of qcr by ten times, this phenomenon being more noticeable for high-conductivity materials and the pressure value is greater than atmospheric one.

The phenomena of ejection of liquid droplets from the cells of the porous structure impair the intensity of heat exchange when a certain boundary heat flux is reached. By choosing the type of structure, this phenomenon can be minimized. The lowest emission was obtained for single-layer meshes with cells more than $0{,}28 \times 10^{-3}$ m. The resulting degraded regimes are similar in their mechanism to the processes occurring when the steam-water mixture moves in pipes that do not have a porous coating. These regimes are characterized by a resistance crisis when frictional resistance begins to decrease in the heated area. This is since due to the strong droplet ejection the liquid consumption is reduced. In the initial stage of the discharge process, droplets turbulizing the process, then at a critical ejection the amount of liquid becomes insufficient to irrigate the heat exchange wall.

Intense drop priming breaks the smooth flow of liquid along the outer surface of the mesh, a film break is observed, which also worsens the influx of fresh portions of relatively cold liquid to the walled two-phase boundary layer. The experimentally chosen porous structures practically eliminated droplet ejection at a given heat flux, which is due to the balancing of the frictional forces of the liquid in the meshes and on the surface of the meshes with droplets and steam flow in meshes and in the circumscribed space.

As a result of disturbance of the balance of operating forces, the amount of incoming liquid becomes insufficient, "dry" spots appear on the heating surface, the wall temperature gradually increases to a certain value and the process proceeds at temperature head (60...80) K. The pulsing mode of supplying the wall with a liquid does not lead to a burn of the surface, although the intensity of heat transfer decreases. However, there are pulsations of wall temperature and associated thermal destructive stresses that shorten the life of the surface. Therefore, it is important to correctly optimize the appearance of the porous structure and avoid high wall overheating with respect to the liquid temperature.

Thus, we carried out the studies of the heat transfer crisis depending on the underheating and flow velocity, the thermal properties of the heating surface, and ejection of liquid droplets from the porous structure. We determined the design principles of combustion chambers and nozzles and calculation of the critical heat flux. The studies have practical significance in the area of the limiting state of the steam generating surface protected by cooling against burning.

Fig. 5 shows a comparative evaluation of the system (4) studies with a curve in a large volume (region 1), thin-film evaporators (region 3), and the area of heat pipes operation (2). The system (4) expands the limit of removal of thermal loads approaching the liquid boiling in a large volume, and in the case of intensifiers, it can also divert large heat fluxes (the shaded part of region 4). As intensifiers of heat exchange, we investigated wavy porous elements with gas-liquid dispersions and an optimized capillary-porous structure; vibrating high-conductor band and flexible turbulator.

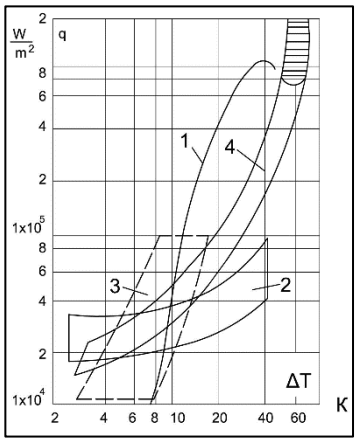

Fig. 5. Influence of heat flux density on wall overheating with respect to water vapor temperature (P = 0.1 MPa): 1 - boiling in a large volume on uncoated surface [5-8,15]; 2 - area of heat pipes operation [9-11]; 3 - area of operation of thin-film evaporators [5]; 4 - studied porous cooling system. Shaded area means application of intensifiers in a porous system [1-4,16].

4 Model of capillary-porous coating for the heating surface limiting state

For the bubble model according to Fig. 3 we consider the solution of the thermoelasticity problem to determine the limiting state of the medium with the help of the example of a brittle coating made of rocks and a metal vapor generating surface (a substrate).

For the thermal destruction of porous coating, we estimate the influence of the specific heat flux q applied to the surface and the time of its action τ to create destructive stresses, the granulometric composition of the husks δ (detachable particles upon destruction), and for the metal, the depth of penetration of the temperature disturbance with destruction of the surface 5 (see Fig.3).

Let's consider the free layer from all sides (an arbitrary shape in plan) 2h thick. To the surface z = + h, starting from the moment of time τ = 0, a constant specific heat flux q is supplied. The bottom surface z = - h and the side edges of the plate are thermally insulated. Equations of thermal conductivity with boundary and initial conditions can be presented in the form:

$$\alpha_w \frac{\partial^2 T}{\partial z^2} = \frac{\partial \mathrm{T}}{\partial \tau},\ \mathrm{T} = 0,\ \tau < 0 \qquad (2)$$

$$\lambda_w \frac{\partial T}{\partial z} = q,\quad z = +h$$

$$\lambda_w \frac{\partial T}{\partial z} = 0,\ z = -h$$

The temperature distribution over the thickness depends on the thermal properties of the material, the heat flux in relation of the time supplied:

$$T\left(\frac{z}{h};\tau\right) = q\left\{\frac{M}{2(c\lambda\rho)_w}\tau + \frac{\frac{3z^2}{h^2}+\frac{6z}{h}-1}{12M} - \frac{4}{\pi^2 M}\ \sum_{n=1}^{\infty}\frac{(-1)^n}{n^2}exp\left[-n^2\frac{\pi^2M^2}{4(c\lambda\rho)_w}\tau\right]\cos\left[\frac{n\pi}{2}\left(\frac{z}{h}+1\right)\right]\right\} \qquad (3)$$

where $M = \frac{\lambda_w}{h}$; n – positive integers.

Knowing the temperature distribution in the plate, we find the thermal tension and compression stresses arising at some time τ at different depths from the surface $\delta_i(h=z_i)$ for a given value of the heat flux q, const. The plate with a variable temperature is in a plane stress state.

4.1 Solution procedure

Setting the limiting values of the compression $\sigma_{comp.stress}$ and tension $\sigma_{tens.stress.}$ stress for each given coating and metal, we obtain the functional dependence of the heat flux q_i required for destruction from the time of delivery and the depth of penetration. Besides, equating the temperatures on the plate surface to the melting point of the coating and the metal, we find the values of the specific heat fluxes necessary for melting the surface layer within a different time interval of their action. Thus, in each case, we obtain the functional dependences of the heat flux qi on the time of its effect on the medium:

- surface melting:

$$q_1 = \frac{\mathrm{T}_f}{\frac{M}{2(c\rho\lambda)_w}\tau+\frac{2}{3M}-\frac{4}{\pi^2 M}\sum_{n=1}^{\infty}\frac{(-1)^n}{n^2}exp\left[-n^2\frac{\pi^2M^2}{4(c\rho\lambda)_w}\tau\right]cosn\pi} \qquad (4)$$

- creation of limiting compression stresses:

$$q_2 = \frac{\frac{(1-\nu)\sigma_{comp.stress}}{\alpha \mathrm{E}}}{\frac{M}{2(c\lambda\rho)_w}\tau+\frac{\frac{3z^2}{h^2}+\frac{6z}{h}-1}{12M}-\frac{4}{\pi^2 M}\ \sum_{n=1}^{\infty}\frac{(-1)^n}{n^2}exp\left[-n^2\frac{\pi^2M^2}{4(c\lambda\rho)_w}\tau\right]\cos\left[\frac{n\pi}{2}\left(\frac{z}{h}+1\right)\right]} \qquad (5)$$

- creation of limiting tensile stresses:

$$q_3 = [(1-\nu)\sigma_{tens.stress}].\,2(c\lambda\rho)_w/(\alpha EM\tau) \qquad (6)$$

For plates made of quartz, granite, teschenite and metal, the functional dependencies q_1, q_2, q_3 were calculated via PC.

5 Mechanism and calculation of the limiting state of heat transfer surfaces. Experimental data analysis

The results of calculations for various coatings are shown in Figure 5-7. In case of a quartz coating, the heat fluxes were calculated for very wide time intervals (10^{-8} ÷ 10^{3}) s. The lower limit of this interval (10^{-8}) s is the relaxation time.

For time intervals of the order of (10^{-8} ÷ 10^{-3}), the ratio for q_1 and q_2 representing hyperbolic type curves in the (q,τ) coordinates, lose physical meaning, since the heat equation was taken as the basis in this problem. To account for the microprocesses in it, you must add a member typed $K' \frac{\partial^2 T}{\partial \tau^2}$.

Since the thermal destruction is a macroprocess, we consider it as taking place over time ($5x10^{-3}$ – 10^{3}). The change in the heat fluxes q_1, q_2, q_3, versus time on the plates made of a teshenite coating is shown in Fig. 5.

If the coatings are destroyed only by compression, a series of curves are obtained, each of which corresponds to a certain thickness of the opening particle. For each value of the heat flux and a certain time interval, we obtain particles with thicknesses δ_1, δ_2 …δ_i.

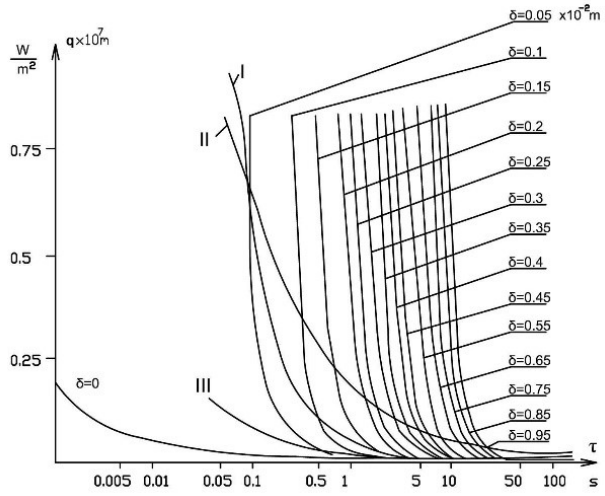

Fig. 5. Dependence of the heat fluxes causing tessite compression stresses depending on the time of action for different thickness of the detached particles: I - tensile stresses sufficient for destruction; II - fusion of the surface; III - destructive thermal compression stresses. Curves II 'and II "for copper and stainless steel almost coincide with curve I in the interval τ = (0,1…1) c.

The maximum thickness of the particles detaching under the action of compression forces for coatings made of quartz and granite is (0.25 - 0.3)$x10^{-2}$ m (see Fig. 7)

The sections of the compression curves (see Fig. 5) determining detachment of particles with thicknesses δ> $0.1x10^{-2}$ m for large heat fluxes and small τ, are screened by the melting curve II, and in the case of small heat fluxes and significant time intervals, by the expansion curve. Moreover, the melting curve of the coating made of quartz is much higher than that of granite explaining its stable brittle fracture.

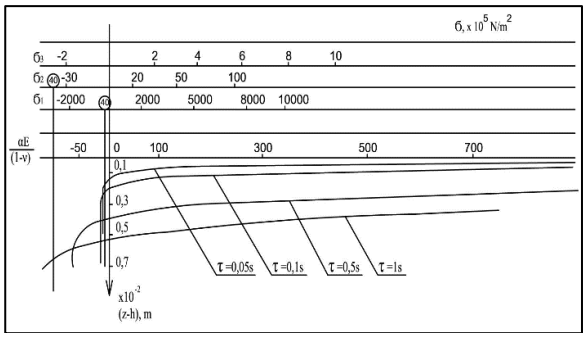

Fig. 6. Stress diagrams for the quartz plate thickness for various heat fluxes and the time of their action: $q_1 = 8.8x10^7$ W/m²; $q_2 = 0.12x10^7$ W/m²; $q_3 = 0.008x10^7$ W/m²; 40 - limiting tensile strength

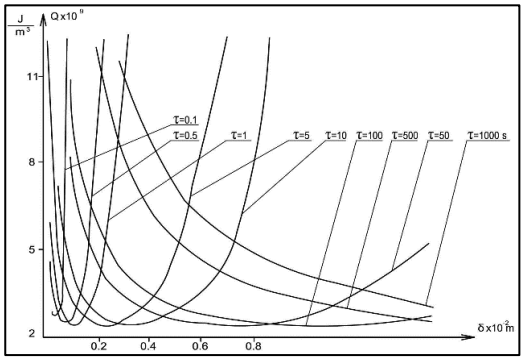

Fig. 7. Change in the specific destruction energy of the granite coating Q depending on δ for different τ. Q = qτ/ δ.

The relationship between compressive stresses and tensile stresses (see Fig. 6) is the stress plots inside quartz platinum for different time intervals from the beginning of the process under consideration. At small τ of the order of 10^{-1} s, only compression stresses arise. Starting from τ ≈ 0.5 s, in a certain region Δ (h - z_i), the compression stress turns into a tensile stress, and for different time intervals they are at different depths from the plate surface. In the transition region of the compressive stress to the tensile stress, the greatest shear stresses of the coating layers will apparently be observed. In time, the shear stresses reach their ultimate values later than the destructive compressive stresses and, obviously, before the maximum tensile stresses. Destruction from compression can occur both at a certain depth (up to $0.3x10^{-2}$ m²) and in a small surface layer δ within a very short time interval τ.

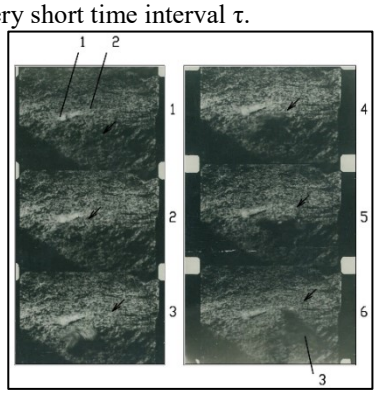

Fig. 8. Fragment of high-speed camera of the tusitic destruction process with a rocket-type flame jet burner with a

specific heat flux equal to $1.2x10^6$ W/m^2. The time for formation of a shelled with a size of $2.5x10^{-3}$ m is 2.2 s. Clearly visible destruction line of "equal opportunities" (shown with an arrow): 1 - capillary-porous coating; 2 - particle (shell) separated from the coating; 3 - destruction line of "equal opportunities". A kinogram of the particles flight within time: τ_1 to τ_6: 1 = 0 s; 2 = 5/1500 s;
3 = 10/1500 s; 4 = 15/1500 s; 5 = 20/1500 s; 6 = 25/1500 s.

Fig. 7 gives the calculation of the specific energy Q of the destruction of a granite coating volume unit. The energy Q is calculated depending on the thickness δ of the particles being detached. The curves have pronounced minimum.

The time of detachment (Fig. 8) of the coarse coating particles determined with a high-speed cinematographic camera SCS-1M, is (0.11...0.47)s and agrees well with the data given (τ_{min} = from 0.1 s and more) (see Fig. 5).

6 Conclusion

A model for generation of vapor bubbles on a solid surface with a porous coating based on kinonegraphographic observations of the liquid boiling internal characteristics is developed.

Experimental installations for determining the: integral (average) heat-exchange characteristics of a capillary-porous cooling system; the functioning scheme and a measuring procedure, the device of a cooling element with tubular arteries perforated pressure plate and microarriers were designed.

Model of the capillary-porous structure of the cooling system was proposed. It was established that the emergence of a boiling crisis is associated with an active increase in the size of the “dry” spot at the base of the bubbles.

The accepted hydrodynamic model of the liquid boiling crisis in a large volume on the surface does not reflect the effect of the thermophysical properties of the wall, although it does occur, which can be explained by the vibrational motion of the steam-liquid interface.

Model of capillary-porous coating for the heating surface limiting state have been accepted. The solution procedure for the governing equation were proposed by the Authors as final relations of the heat flux qi on the time of its effect on the medium were presented.

The heat fluxes applied to the surface are determined, the time of their action to create destructive stresses, the dimensions of the detached particles and the depth of the temperature wave penetration into the substrate. The heat fluxes were calculated from the time of the steam germ explosive appearance (10^{-8} s), i.e. from the time of relaxation to the time describing the macroprocess. The relationship in the destruction process is established only with the compression stress, melting, or tensile stress. The dimensions of the detached particles are confirmed with a high-speed camera.

The performed study shows that in case of a quartz coating, the heat fluxes changes in a very wide time intervals ($10^{-8} \div 10^3$) s. The lower limit of this interval (10^{-8}) s is the relaxation time.

A very useful graph is obtained when coatings are destroyed only by compression. Each line corresponds to a certain thickness of the opening particle. For each value of the heat flux and a certain time interval particles with thicknesses δ_1, δ_2 …δ_i are obtained.
The relationship between compressive stresses and tensile stresses inside quartz platinum for different time intervals from the beginning of the process is provided. At small τ of the order of 10^{-1} s, only compression stresses arise. Starting from $\tau \approx 0.5$ s, in a certain region Δ (h - z_i), the compression stress turns into a tensile stress, and for different time intervals they are at different depths from the plate surface. Destruction from compression can occur both at a certain depth (up to $0.3x10^{-2}$ m^2) and in a small surface layer δ within a very short time interval τ.

References

1. Polyaev V.M., Genbach A.A., 1995, Methods of Monitoring Energy Processes, Experimental Thermal and Fluid Science, International of Thermodynamics, Experimental Heat Transfer and Fluid Mechanics, Avenue of the Americas, New York, USA, Vol. **10**, 273-286
2. Polyaev V.M., Genbach A.A., 1991, A Limit Condition of a Surface at Thermal Influence, Teplofizika Vysokikh Temperatur, 29, 923-934, (in Russian)
3. Genbach A.A., Jamankylova N.O., Bakic Vukman V., 2017, The processes of Vaporization in the Porous Structures Working with the Excess of Liquid, *Thermal Science 1*, Vol **21**, 363-373
4. Genbach A.A., Olzhabayeva K.S., Iliev I.K., 2016, Boiling Process in oil Coolers on Porous Elements, *Thermal Science 5*, Vol. **20**, 1777-1789
5. Jamialahmadi M., et al., 2008, Experimental and Theoretical Studies on Subcooled Flow Boiling of Pure Liquids and Multicomponent Mixtures, *Intern. J Heat Mass Transfer*, 51, 2482-2493
6. Ose Y., Kunugi T., 2011, Numerical Study on Subcooled Pool Boiling, Programme in Nuclear Science and Technology, 2, 125-129
7. Krepper E., et al., 2007, CFD Modeling Subcooled Boiling-Concept, Validation and Application to Fuel Assembly Design, Nuclear Engineering and Design, 7, 716-731
8. Ovsyanik A.V., 2012, Modeling of Processes of Heat Exchange at Boiling Liquids (in Russian), Gomel State Technical University named after P.O., Sukhoy, Gomel, Belarus
9. Alekseik O.S., Kravets V.Yu, 2013, Physical Model of Boiling on Porous Structure in the Limited Space, Eastern-European *Journal of Enterprise Technologies*, 64 4/8, 26-31
10. Polyaev V.M., Mayorov V.A., Vasilev L.L. 1998, Hydrodynamics and heat exchange in porous structural elements of aircrafts. Mechanical engineering, 168 p. (in Russian)

11. Kovalev S.A., Solovev S.L, 1989, Evaporation and condensation in heat pipes, Science, 112 p. (in Russian)
12. Kupetz M., Jeni Heiew E., Hiss F., 2014, Modernization and extension of the life of steam turbine power plants in Eastern Europe and Russia, Heat power engineering. 6, 35-43. (in Russian)
13. Grin E.A., 2013, The possibilities of fracture mechanics in relation to the problems of strength, resource and justification for the safe operation of thermal mechanical equipment, Heat power engineering, 1. 25-32. (in Russian)
14. Shklover E.G. Experimental Study of Heat Transfer from Porous Surface in Pool and Forced – Convection Boiling at Low Pressures, Phase Change Heat Transfer ASME. 1991. Vol. **159**, 75-80
15. Barthau G. Active nucleation site density and pool boiling heat transfer, *Int. J. Heat Mass Transfer. 1992*, V. **35**, 271-278
16. Polyaev V.M., Genbach A.A., An experimental study of thermal stress in porous materials by methods of holography and photoelasticity, Experimental Thermal and Fluid Science, Avenue of the Americas, New York, USA, - 1992. Vol. 5, №6, pp. 697-702